Through-Bonds and Through-Space Solid-State NMR Correlations at Natural Isotopic Abundance: Signal Assignment and Structural Study of Simvastatin

Jiri Brus*,† and Alexandr Jegorov‡

Institute of Macromolecular Chemistry, Academy of Sciences of the Czech Republic, Heyrovsky sq. 2, 162 06 Prague 6, Czech Republic, and IVAX Pharmaceutical sro, Research Unit, Branisovska 31, 370 05 Ceske Budejovice, Czech Republic

Received: January 14, 2004; In Final Form: February 17, 2004

Through-bond and through-space solid-state NMR correlation experiments at natural isotopic abundance (refocused cross-polarization incredible natural abundance double quantum transfer experiment (CP-INADEQUATE), $^{1}H-^{13}C$ HETCOR, $^{1}H-^{13}C$ magic-angle spinning *J* heteronuclear multiple-quantum coherence (MAS-*J*-HMQC)) are presented on a moderately sized molecule of simavastatin ($C_{25}H_{38}O_5$). Refocused $^{13}C-^{13}C$ CP-INADEQUATE with an optimized performance of high-power decoupling provides full correlation spectrum within a day of acquisition. Complete unambiguous ^{1}H and ^{13}C signal assignment was achieved by $^{1}H-^{13}C$ MAS-*J*-HMQC and dipolar heteronuclear correlation spectroscopy. Dipolar $^{1}H-^{13}C$ correlation with Lee−Goldburg CP (LG-CP) was used to promote long-range polarization transfer. More than 80 heteronuclear contacts were detected in 2D spectra measured with gradually increasing LG-CP. The majority of these interactions reflects polarization transfer between neighboring structural units. Approximately 30 cross peaks correspond to desired long-range correlation, and 20 of them can be unambiguously used to derive interatomic distances. Formation of additional coherences indicating $^{1}H-^{1}H$ polarization transfer was observed applying standard Hartmann−Hahn on-resonance CP as a mixing period in 2D HETCOR. No sharp distance border between inter- and intramolecular correlations was found by careful analysis of X-ray diffraction data. Intermolecular $^{1}H-^{13}C$ contacts correspond to a polarization transfer range of 3−5 Å. Short-range intermolecular interactions (3.0−3.3 Å) are indicated by NMR aggregation shifts. In many cases, correlation signals must be considered as a contribution of both inter- and intramolecular polarization transfer events. High selectivity and good resolution of 2D LG-CP HETCOR restricts the size of the mutually interacting spin system reflected by a single cross peak. As the number of protons interacting with one carbon does not usually exceed 3−4, the observed dipolar oscillations of correlation signals can be analyzed with respect to heteronuclear dipolar couplings. The obtained $^{1}H-^{13}C$ and $^{1}H-^{1}H$ contacts used in conjunction with ^{13}C and ^{1}H NMR aggregation shifts thus appear to be a practical and efficient tool to determine conformation and mutual orientation of well-organized molecules within crystal at natural isotopic abundance.

Introduction

Advanced techniques of solid-state NMR spectroscopy nowadays provide a wide range of qualitative and quantitative structural and dynamic data, which are of serious interest to methodological development as well as to application, especially for bio-organic solids. The majority of these recently developed techniques based on dipole−dipole interaction between heteronuclei (i.e., recoupling experiments, double cross polarization (CP), etc.) require selective or uniform isotopic enrichment. The requirement of labeled materials, however, renders application of these techniques impractical for the solution of some academic and industrial problems where synthetic effort necessary to selectively or uniformly label the molecules can be nearly daunting. Recent advances in NMR spectrometers and probeheads design improved sensitivity and resolution in such way that a basic experimental concept intended for labeled materials can be partially used also for systems at natural isotopic abundance.

The first step for structure determination is unambiguous signal assignment for which through-bond correlation techniques are usually applied due to their unique selectivity. There are two-dimensional (2D) experiments such as correlation spectroscopy (COSY),[1] heteronuclear multiple-quantum coherence (HMQC),[2] heteronuclear multiple-bond correlation (HMBC), and incredible natural abundance double quantum transfer experiment (INADEQUATE),[3,4] which are frequently used in liquid-state NMR. In the solid state, these techniques are rare since the scalar couplings between the adjacent nuclei are significantly weaker than the dipolar couplings, which are thus preferred. That is why the first solid-state correlation technique based on *J* coupling, known as total through-bond correlation spectroscopy (TOBSY), was reported in 1996 by Meier et al.[5,6] During the following years, heteronuclear $^{1}H-^{13}C$ magic angle spinning (MAS)-*J*-HMQC (HSQC)[7,8] and homonuclear $^{13}C-^{13}C$ CP-INAEQUATE[9] experiments were developed and demonstrated not only on labeled systems but also on small-size organic compounds at natural isotopic abundance. Significant sensitivity enhancement was achieved by refocused CP-INADEQUATE,[10] allowing detection of in-phase cross peaks. For example, four-day acquisition in a 7-mm rotor (300-MHz spectrometer, 300 mg of sample) provides a high-quality

* To whom correspondence may be addressed. E-mail: brus@imc.cas.cz. Telephone: +420 296 809 380. Fax: +420 296 809 410.
† Academy of Sciences of the Czech Republic.
‡ IVAX Pharmaceutical sro.

10.1021/jp0498163 CCC: $27.50
Published on Web 04/10/2004

spectrum of native crystalline cellulose and allows resolution and signal assignment for both I_α and I_β allomorphs.[11] Newly developed UC2QF COSY (uniform-sign cross-peak double-quantum-filtered correlation spectroscopy) leads to a highly resolved symmetric $^{13}C-^{13}C$ correlation spectrum of a moderately sized spin system within two weeks of acquisition[12] (unlabeled vitamin-d_3, $C_{27}H_{43}O$ with two inequivalent molecules in unit cell). Quite recently reported transverse-dephasing optimized refocused CP-INADEQUATE,[13] providing nearly five times the improvement in sensitivity, is a very promising tool, which can be applicable also for moderately sized unlabeled molecules. Nevertheless, up to now, there are only a few examples of natural abundance ^{13}C correlation experiments on molecules with more than a dozen of carbon sites.

The second step in three-dimensional structure elucidation is the determination of geometrical constraints, mainly interatomic distances. This is usually achieved by multidimensional experiments in which correlation between heteronuclei such as $^{13}C-^{13}C$, $^{13}C-^{15}N$, etc. is mediated by through-space dipolar interactions. For instance, global fold of SH3 (α-spectrin src-homology 3 domain) has been recently calculated on the basis of a large set of $^{13}C-^{13}C$ and $^{15}N-^{15}N$ inter-residue restraints derived from proton-driven spin diffusion (PDSD).[26] However, in unlabeled systems, we must focus on ^1H spins which high magnetogyric ratio and high isotopic abundance allow tracing of interatomic contacts theoretically up to 4−5 Å. Recent improvement in homodecoupling techniques employing the Lee−Goldburg (LG) approach[14] (e.g., FSLG, frequency switched,[15] or PMLG, phase modulated)[16] leads to a detection of 2D $^1H-^{13}C$ correlation spectra with resolution sufficient to separate correlation signals. Unambiguous ^1H signal assignment is achieved by $^1H-^{13}C$ MAS-*J*-HMQC or $^1H-^{13}C$ HETCOR in which polarization transfer occurs during a very short time. The efficient suppression of unwanted $^1H-^1H$ spin exchange during CP achieved by LG spin-lock (LG-CP) leads to oscillatory behavior of ^{13}C magnetization reflecting strength of $^1H-^{13}C$ dipolar coupling. It has been reported that this time evolution can be evaluated with respect to interatomic distance.[17,18] Long-range $^1H-^{13}C$ correlations have been recently successfully used to establish the stacking of molecules in the fully labeled chlorophyll *a*/H_2O assembly.[23]

In this contribution, we present an initial solid-state NMR study of structure and dynamic of simvastatin ($C_{25}H_{38}O_5$) at natural isotopic abundance. Simvastatin as an active metabolite (simvastatin acid) inhibits 3-hydroxy-3-methylglutaryl coenzyme A (HMG-CoA) reductase, an enzyme that is necessary in an early step of the cholesterol synthesis. Although in this case X-ray structure has been determined,[21] solid-state NMR-derived structures and dynamic behavior are required for further formulation of other related drugs due to the low tendency of this substance to form a single crystal suitable for X-ray diffraction studies. The aim of our work was an evaluation of the ability of solid-state NMR techniques to determine on an unlabeled system sufficient structural information to elucidate conformation and aggregation of the molecules.

First, we demonstrate the discrimination of main functional groups employing editing techniques based on dipolar and *J*-couplings (CPPI, cross-polarization polarization-inversion,[19] and SoS-APT, solid-state attached proton test,[20] respectively). Complete signal assignment is obtained by optimized refocused CP-INADEQUATE and a series of $^1H-^{13}C$ correlation experiments. Subsequently, we focus to the observation of long-range $^1H-^{13}C$ contacts evolved under LG-CP conditions. Detection of additional $^1H-^{13}C$ coherences created during Hartman−Hahn cross polarization is discussed with respect to formation of $^1H-^1H$ polarization coherences providing further geometrical constraints. Comparison of solid-state NMR results with known X-ray diffraction data[21] is a necessary clue for further structural study of unknown materials. The longest-detected interatomic $^1H-^{13}C$ distance and the number of mutually interacting spins reflected by a single cross peak as well as discrimination of inter- and intramolecular contacts is discussed.

CHART 1. Molecular Structure of Simvastatin with Numbering of All ^{13}C Sites

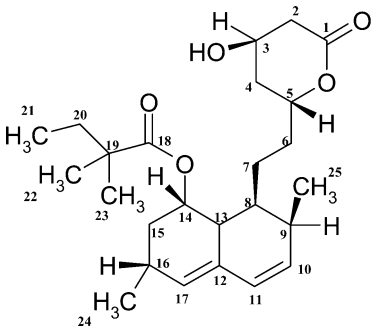

Experimental Section

Sample. To a solution of simvastatin (BIOCON, India Ltd.) in acetone (1.1 g per 3.5 mL) was added *n*-heptane (6.5 mL). The mixture was allowed to stand overnight, and the resulting crystals were washed with *n*-heptane. A powdered sample was used for further NMR analysis without any purification.

NMR Experiments. NMR spectra were measured with a Bruker Avance 500 NMR spectrometer (Karlsruhe, Germany, 2003) in a 4-mm ZrO_2 rotor. MAS speed was 11 kHz in all cases, nutation frequency of the $B_1(^{13}C)$ field was 62.5 kHz, and repetition delay was 2−4 s. The polarization−inversion period for the CPPI experiment[19] was 55 μs. Both evolution periods in the SoS-APT experiment[20] were 5.5 ms. Evolution delays in refocused CP-INADEQUATE[10] were 5.4 ms, and 128 t_1 increments consisting of 320 scans were collected (total acquisition time was 23 h). TPPM (two-pulse phase-modulated) decoupling[22] was applied during evolution and both detection periods. The phase modulation angle was 15°, and the flip−pulse length was 4.8 μs. Applied nutation frequency of the $B_1(^1H)$ field was $\omega_1/2\pi = 89.3$ kHz. For recording of the $^1H-^{13}C$ MAS-*J*-HMQC[7] spectrum, a FSLG decoupling field strength of $\omega_1/2\pi = 100$ kHz was applied during both evolution delays ($\tau = 1.4$ ms) and detection t_1 period consisting of 128 increments each made of 320 scans. The same intensity of the $B_1(^1H)$ field was used for measurement of $^1H-^{13}C$ HETCOR[17,23] spectra. Because of higher sensitivity, 64−80 scans were sufficient to reach an acceptable signal-to-noise ratio. On-resonance CP and LG-CP ranging from 0.05 to 2.0 ms were used as mixing periods. Intensity of the $B_1(^1H)$ field for CP was $\omega_1/2\pi = 62.5$ kHz. The ^{13}C scale was calibrated with glycine as an external standard (176.03 ppm, low-field carbonyl signal). The external standard l-[U$-^{13}C$, ^{15}N] Ala was used for calibration of the ^1H scale. A ^1H chemical shift of Hβ was set to 1 ppm, and the proton chemical shift scale was corrected to achieve a ^1H chemical shift of Hα and NH_3^+ signals ca. 3.8 and 9.2 ppm, respectively.

Results and Discussion

Simvastatin, or (1*S*,3*R*,7*S*,8*S*,8a*R*)-8-{2-[(2*R*,4*R*)-4-hydroxy-oxo-3,4,5,6-tetrahydro-2*H*-pyran-2-yl]ethyl}-3,7-dimethyl-1,2,3,7,8,8a-hexahydronaphthalen-1-yl 2,2-dimethybutanoate, $C_{25}H_{38}O_5$ (Chart 1), provides an example of a highly organized

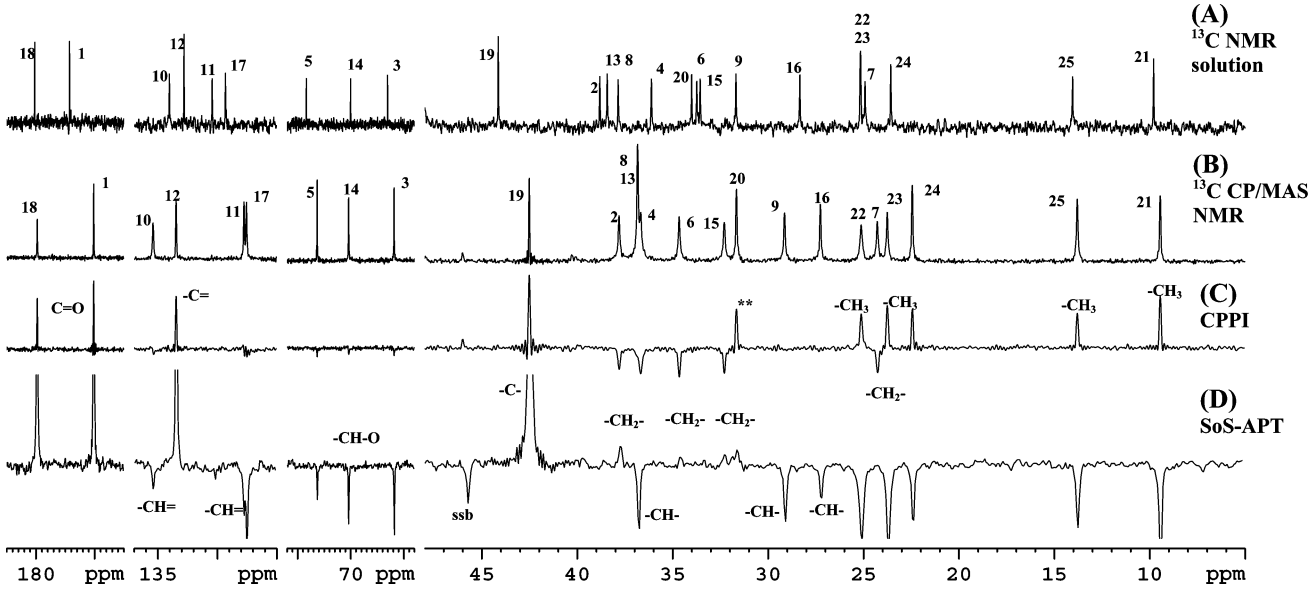

Figure 1. ^{13}C NMR (solution, 3072 scans, A); ^{13}C CP/MAS NMR (1-ms contact time, 64 scans, B); CCPI (55-μs polarization inversion time, 128 scans, C); and SoS-APT (5.5-ms evolution time, 512 scans, D) spectra of simvastatin. (Signal assignment is introduced in Chart 1).

crystalline organic solid. As simvastatin crystallizes in a unit cell in which all molecules have equivalent conformations, there is only one set of ^{13}C NMR signals corresponding to carbon atoms and the line-width of all signals ranges between 20 and 12 Hz. Consequently, in a ^{13}C CP/MAS NMR spectrum, we resolve all ^{13}C sites while only signals of two structure units overlap. Because of the significant conformation changes and/or molecular packing caused by crystallization forces (noncovalent bonding such as hydrogen bonds, $\pi-\pi$ interactions, etc.), signal assignment obtained from solution NMR cannot be simply applied for the crystalline material. The differences in liquid- and solid-state ^{13}C NMR chemical shifts are demonstrated in parts A and B of Figure 1.

Spectral Editing. Before complete signal assignment, we discriminated carbon atoms according to number of attached protons applying editing techniques which are based either on differences in CP dynamics or evolution of carbon coherences under the influence of carbon-proton scalar couplings. As the former experiment is affected by segmental motion modulating dipolar couplings and may fail at high magnetic field and fast spinning regime,[24] the obtained results must be carefully evaluated. (In general, C and CH_3 signals should be positive, CH_2 negative, and CH signals suppressed in CPPI spectra.) Using 55 μs of a polarization inversion period (optimized value), we observe in a CPPI spectrum an unexpected positive signal with full intensity reflecting high segmental motion of the flexible part of the molecule (Figure 1C, signal marked by asterisks). The latter technique, which is insensitive to molecular motion, provides very straightforward results. (With optimized evolution delays, the signals of nonprotonated and CH_2 carbons are positive while signals of CH and CH_3 units are negative.)

Unfortunately, fast transverse dephasing of carbon coherences during long-time evolution of $^1H-^{13}C$ J couplings leads to suppression of CH_2 resonances. Nevertheless, all CH_2 signals were detected (Figure 1D) and provide identification of the unexpected positive signals to the CH_2 structure unit in which the effective strength of $^1H-^{13}C$ dipolar coupling is motionally reduced to be comparable with dipolar couplings in rapidly rotating methyl. Such fast rotation motion can be expected only for an ester tail (units 18−23), as clearly proved by $^1H-^{13}C$ dipolar spectra, which will be introduced later. As the CPPI experiment is in some cases confusing, the SoS-APT technique providing accurate data must be applied to check the results, although some CH_2 signals may be completely lost, e.g., CH_2 unit at 24 ppm, Figure 1D).

Through-Bond Correlation (CP-INADEQUATE). For a complete signal assignment, it is necessary to employ 2D correlation techniques. $^{13}C-^{13}C$ connectivity can be directly probed by refocused CP-INADEQUATE, the primary limitation of which at natural isotopic abundance is, however, low sensitivity. As correlation spectroscopy relies on pairs of nuclei to be active, only 1% ^{13}C isotope natural concentration leads to a decrease in sensitivity of the technique by 4 orders of magnitude as compared to correlation experiments on enriched materials.

By omission of isotopic enrichment of systems, sensitivity in the solid state is usually enhanced by MAS, CP, and high-power decoupling. In CP-INADEQUATE especially, efficiency of high-power heteronuclear decoupling, under which both detection and evolution periods occur, significantly affects the resulting signal-to-noise ratio. This fact requires careful optimization of decoupling performances directly on the studied sample at particular conditions (temperature and spinning speed). Simple observation of line width and intensity of signals with respect to decoupling parameters, however, is not useful for narrow signals with a half width less than 20 Hz because one limiting factor of resolution is acquisition time ($aq_{max} = 50$ ms). In addition, it has been mentioned quite recently that even once the limiting line width had been reached, decoupling sequences continue to act strongly on transverse-dephasing times.[13] It has been shown that an actively developed and optimized decoupling sequence (eDROOPY)[25] can increase the coherence lifetimes up to a factor of 2, although there is no difference in the 1D spectra.[13]

We optimized the TPPM sequence starting from the best result obtained for the Cα signal of glycine at 11 kHz (pulse length was 4.9 μs). The phase modulation angle was kept constant, at 15°, as was the decoupling field strength, $\omega_1^H/2\pi = 89.3$ kHz. For selected signals, the pulse length was optimized by using a spin−echo procedure to yield as long a transverse-dephasing lifetime as possible. Although a very small modification of decoupling pulse length (±0.05−0.1 μs) causes almost negligible differences in intensity and line width of selected signals (less than 2 and 1%, respectively), optimization of

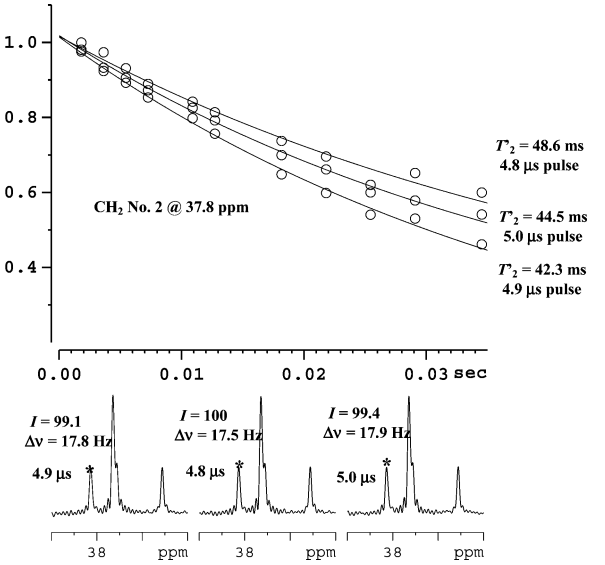

Figure 2. The transverse-dephasing curves obtained by using spin−echo pulse sequence for a CH_2 (2) signal at various lengths of the decoupling pulse (A) and corresponding ^{13}C CP/MAS NMR spectra (B). The selected signal is marked by an asterisk. I, $\Delta\nu$ and T'_2 correspond to intensity, line width and transverse-dephasing constant, respectively.

decoupling sequence saves more than 14% of coherence (Figure 2). An additional increase in T'_2 can be expected with increasing strength of the decoupling field; however, we are limited by total time during which the decoupling field is on (70 ms). Dissipation of a higher amount of energy would require intensive cooling and longer repetition delay.

An excellent CP-INADEQUATE spectrum was acquired within 23 h of measurement (Figure 3), while satisfactory results had been obtained even after 16 h. A high signal-to-noise ratio is clearly apparent from single-quantum projection. Full correlation was obtained for all saturated (aliphatic) structure units for which evolution delays corresponding to $^1/_4(^1J_{C-C})$ were optimized (τ = 5.4 ms for ca. $^1J_{C-C}$ = 46 Hz; synchronized with spinning speed). As scalar couplings including unsaturated carbons are larger, signals correlating corresponding groups are not fully evolved. For a full evolution of these correlation signals, the estimated evolution period should be shorter, τ = 3.4 ms, for $^1J_{C-C}$ = 72 Hz. Because of the limited number of t_1 increments resulting in partly reduced resolution in double-quantum dimension, the previous distinction of main function groups is a helpful clue for accurate tracing of $^{13}C-^{13}C$ connectivity. This connectivity was nicely traced for the ester part of the molecule from carbon atoms CO (18) to CH_3 (23), from CO (1) to CH_3 (25), from CH_3 (25) to (24) through CH (9), (8), etc., and finally from ═CH− (17) to ═CH− (12). The absence of correlation between saturated and unsaturated ═CH− carbons leaves signals at 127.55 and 127.76 ppm corresponding to carbon atoms (17) and (12) unassigned. The final solution was achieved in series of $^1H-^{13}C$ HETCOR experiments as discussed below.

Heteronuclear $^1H-^{13}C$ Correlation (MAS-J-HMQC, FS-LG HETCOR). Following almost complete ^{13}C assignment, ^1H resonances were assigned and interatomic contacts determined by $^1H-^{13}C$ heteronuclear correlation spectroscopy. Although the resolution of ^1H resonances obtained as a projection of 2D spectra (parts A and B of Figure 4) is not still comparable with resolution achieved in liquids, all ^1H signals are nicely resolved in 2D spectrum.

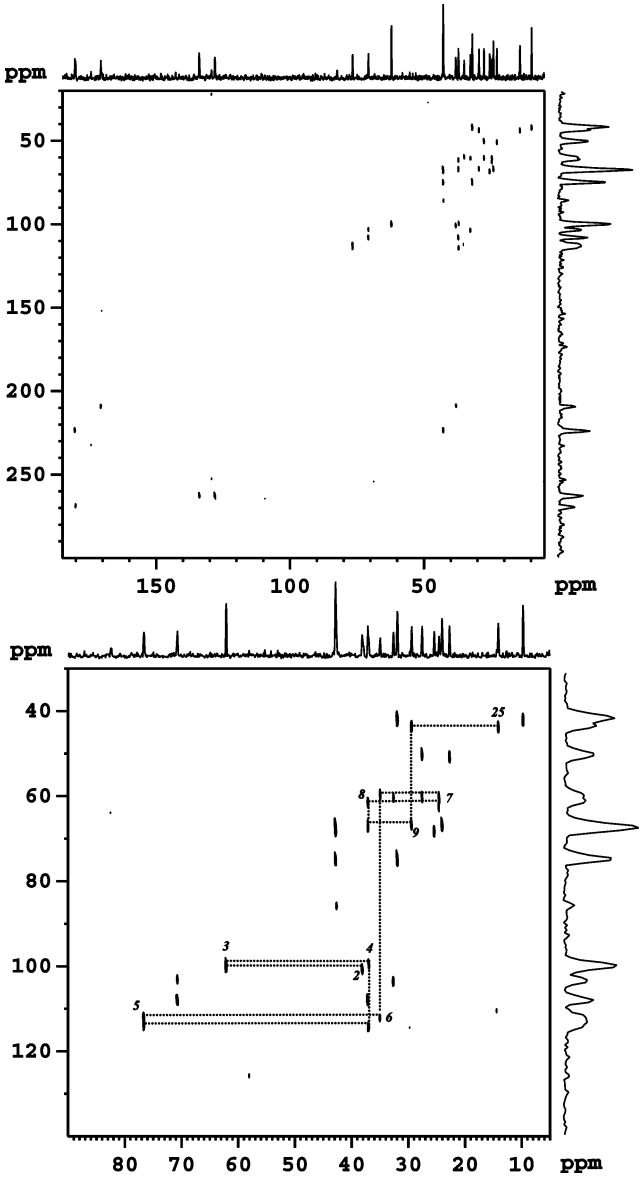

Figure 3. Refocused $^{13}C-^{13}C$ CP-INADEQUATE spectrum acquired with a 4-mm DR CP/MAS probe with a full rotor and with 320 scans for each of the 128 increments in t_1. Full spectral range (A); aliphatic region (B). Single- and double-quantum projections are depicted in the upper and right side of 2D spectra.

The line width of the signals processed without any window function is ca. 0.5−0.6 ppm. This makes possible to exactly assign chemical shifts of all directly bonded protons. Liquid- and solid-state NMR chemical shifts are summarized in Table 1.

By use of the listed assignment, "aggregation" shifts, $\Delta = \delta_{liq} - \delta$, reflecting differences in electronic structure between monomeric (dissolved) and aggregated (crystallized) molecules were calculated. The largest upfield aggregation ^{13}C shifts Δ = 3.61 and 2.39 ppm were detected for carbonyl carbon (1) and CH═ (17), respectively, and the largest downfield shift Δ = −1.87 ppm corresponding to CH═ (10) indicates sites that are probably involved in noncovalent bonding.

From the point of view of selectivity of polarization transfer, it was found that $^1H-^{13}C$ MAS-*J*-HMQC and $^1H-^{13}C$ HETCOR experiments are nearly comparable. By use of 100 μs of on-resonance CP, cross peaks reflecting long-range correlation are almost suppressed and can be easily distinguished from direct one-bond correlation signals. On the other hand, also the

TABLE 1: Solution and Solid-State ^{1}H and ^{13}C NMR Chemical Shifts, δ, and Their Differences, $\Delta = \delta_{liq} - \delta$

	solid-state NMR		liquid-state NMR		differences	
no.	δ (^{13}C), ppm	δ (^{1}H), ppm	δ_{liq} (^{13}C), ppm	δ_{liq} (^{1}H), ppm	Δ (^{13}C), ppm	Δ (^{1}H), ppm
1	170.66		174.27		3.61	
2	38.31	3.24	38.82	2.7	0.51	−0.54
2′		1.91		2.5		0.59
3	62.35	4.53	63.07	4.24	0.72	−0.29
4	37.17	1.71	36.12	1.87	−1.05	0.16
4′		0.83		1.71		0.88
5	76.83	4.41	78.38	4.57	1.55	0.16
6	35.16	0.64	33.84	1.35	−1.32	0.71
6′		1.31		1.86		0.55
7	24.78	1.44	24.92	1.37	0.14	−0.07
7′		0.55		1.37		0.82
8	37.34	1.7	37.86	1.62	0.52	−0.08
9	29.65	3.09	31.68	2.38	2.03	−0.71
10	135.91	6.09	134.04	5.78	−1.87	−0.31
11	128.26	6.06	129.33	5.94	1.07	−0.12
12	133.98		132.8		−1.18	
13	37.34	1.7	38.43	2.28	1.09	0.58
14	70.91	4.96	70.04	5.3	−0.87	0.34
15	32.80	2.03	33.56	1.87	0.76	−0.16
15′		1.55		1.87		0.32
16	27.76	2.35	28.34	2.39	0.58	0.04
17	128.05	5.47	130.44	5.45	2.39	−0.02
18	180.28		180.22		−0.14	
19	43.02		44.14		1.12	
20	32.16	1.23	34.01	1.52	1.85	0.29
21	9.95	0.6	9.78	0.77	−0.23	0.17
22/23[a]	25.52	0.73	25.15	1.06	−0.53	0.33
22/23[a]	24.25	0.81	25.15	1.06	0.90	0.25
24	22.95	0.65	23.57	1.01	0.62	0.36
25	14.30	0.50	14.04	0.83	−0.34	0.33

[a] The differences between C23/C22 and H23/H22 are not resolved in solution. The estimated errors for the solid-state NMR shift of 0.02 ppm for ^{13}C and 0.08 for ^{1}H as followed from two repeated experiments.

intensities of signals of highly mobile methyl groups (22 and 23) are significantly reduced (Figure 4A). Of-course ^{1}H−^{13}C MAS-*J*-HMQC experiment provides unique selectivity; however, because of lower sensitivity, experimental time must be increased by a factor ca. 1.5−2. In contrast, using off-resonance LG-CP (100 μs), we observe formation of additional coherences. During the LG-CP, an off-resonance RF field locks proton spins in the rotating frame along the axis containing angle 54.7° with the direction of static magnetic field, while carbon spins are locked on resonance in the *xy* plane. In this way, heteronuclear spin locking is achieved with simultaneous suppression of ^{1}H−^{1}H flip flops. Consequently, ^{1}H polarization is selectively transferred to carbon atoms.

The suppression of strong ^{1}H−^{1}H dipolar interactions apparently increases the efficiency of ^{1}H−^{13}C polarization transfer in a rigid pair of nuclei, and consequently, the intensity of corresponding long-range correlation signals is enhanced (Figure 4B, signals are marked by arrows). Even using a very short polarization transfer time (50 μs), selectivity of the experiment is not quite improved and unwanted signals are still apparent. The differences in efficiency of polarization transfer during on-resonance and LG-CP are reflected in a pattern of ^{1}H projections. While suppression of ^{1}H−^{1}H spin diffusion enhances efficiency of polarization transfer between rigid structural units (e.g., H3−C4) as a result of restricted number of other polarization transfer pathways, polarization transfer is less effective in highly mobile (rotating) methyl groups. It implies that fast ^{1}H−^{1}H flip flops within rotating methyl groups can partly compensate motional weakening of ^{1}H−^{13}C dipolar interactions.

From the presented 2D spectra, it is clear that all CH_2 protons, except rapidly moving methylene unit (20) in the ester part of the molecule, are nonequivalent, reflecting various shielding in "axial" and "equatorial" position in cycles as well as in short $-(CH_2)_2-$ chains. The most pronounced nonequivalence (1.33 ppm) is observed for the CH_2 unit (H2, H2′) in a lacton cycle. This difference in ^{1}H NMR chemical shifts is much larger than observed in solution (0.2 ppm), reflecting significant changes in conformation and/or participation in formation of noncovalent bonding in the solid state. In addition, ^{1}H chemical shifts provide better resolution of CH═ units. The difference in ^{13}C NMR chemical shift of CH═ (C11) and (C17) is 0.2 ppm, while they both differ about 0.6 ppm in the ^{1}H NMR chemical shift.

In general, these large differences in ^{1}H NMR chemical shifts and nonequivalence of CH_2 protons indicate the possibility to selectively detect long-range ^{1}H−^{13}C polarization transfers between remote atoms if ^{1}H−^{1}H spin exchange during CP will be suppressed by LG ^{1}H spin lock. In 2D ^{1}H−^{13}C LG-CP HETCOR spectra measured with increasing spin-lock time, formation of coherences reflecting long-range ^{1}H−^{13}C dipolar through-space interactions is quite pronounced. Cross peaks correlating CH═ protons (H11) and (H17) with carbon atoms CH (C9) and (C16), respectively, finally complete assignment of ^{13}C and ^{1}H NMR signals in this system (Figure 5A, signals marked by arrows).

Long-Range ^{1}H−^{13}C Correlation. The subsequent step for structure analysis is the selection of unambiguously assigned long-range heteronuclear coherences containing required structure information. Recently, it has been shown that protons in CH_3 groups can transfer magnetization over considerable distances, providing thus an attractive route to the detection of long-range transfer events.[23] Although the resolution in ^{1}H dimension is not perfect, the most upfield shifted methyl protons (H25) provide a useful probe into the longest polarization pathways. In 2D spectra measured with long mixing times of 900 μs and 2 ms (parts B and C of Figure 5) for a rigid part of the molecule (i.e., excluding rapidly moving ester tail), we trace correlation from CH_3 protons (H25) to carbon atoms (C9), (C10), (C11), (C6), and finally (C1).

As ^{1}H magnetization transverse dephasing of CH or CH_2 groups is faster than that of CH_3 moieties, the correlation signal between (H25) and (C6) becomes well resolved at longer mixing times (Figure 5C). Not only CH_3 protons transfer magnetization over a relatively large distance. We observe polarization transfer from well-resolved CH−O (H14) to carbon atoms (C13), (C15), (C18), (C19), and finally (C24). The longest polarization transfer pathway 4.2−4.6 Å (H25−C1, H3−C6, extracted from X-ray diffraction data, Figure 6) is in accord with the previously reported value for the longest ^{1}H−^{13}C contact detected during LG-CP contact time 2 ms.

The slightly upfield shifted position of the expected (H2−C3) correlation signal is surprising. The position in the ^{1}H dimension exactly indicates polarization transfer from tbe hydrogen atom (H9); however, its shortest distance, 5.1 Å, from (C3) is too large to evolve this coherence during short LG-CP (100 μs, Figure 4B). There is no other identified proton which could affect shape and the position of the correlation signal by this way except close −OH proton (ca. 1.9 Å; see Figure 6). Although we could identify very weak interaction of this hydroxyl proton with carbonyl carbon (C18) this explanation seems to be unlikely, because the ^{1}H NMR shift ca. 3.2 ppm does not correspond to usual chemical shift of hydrogen bonded hydroxyl protons. In this case this hydrogen bonding must be

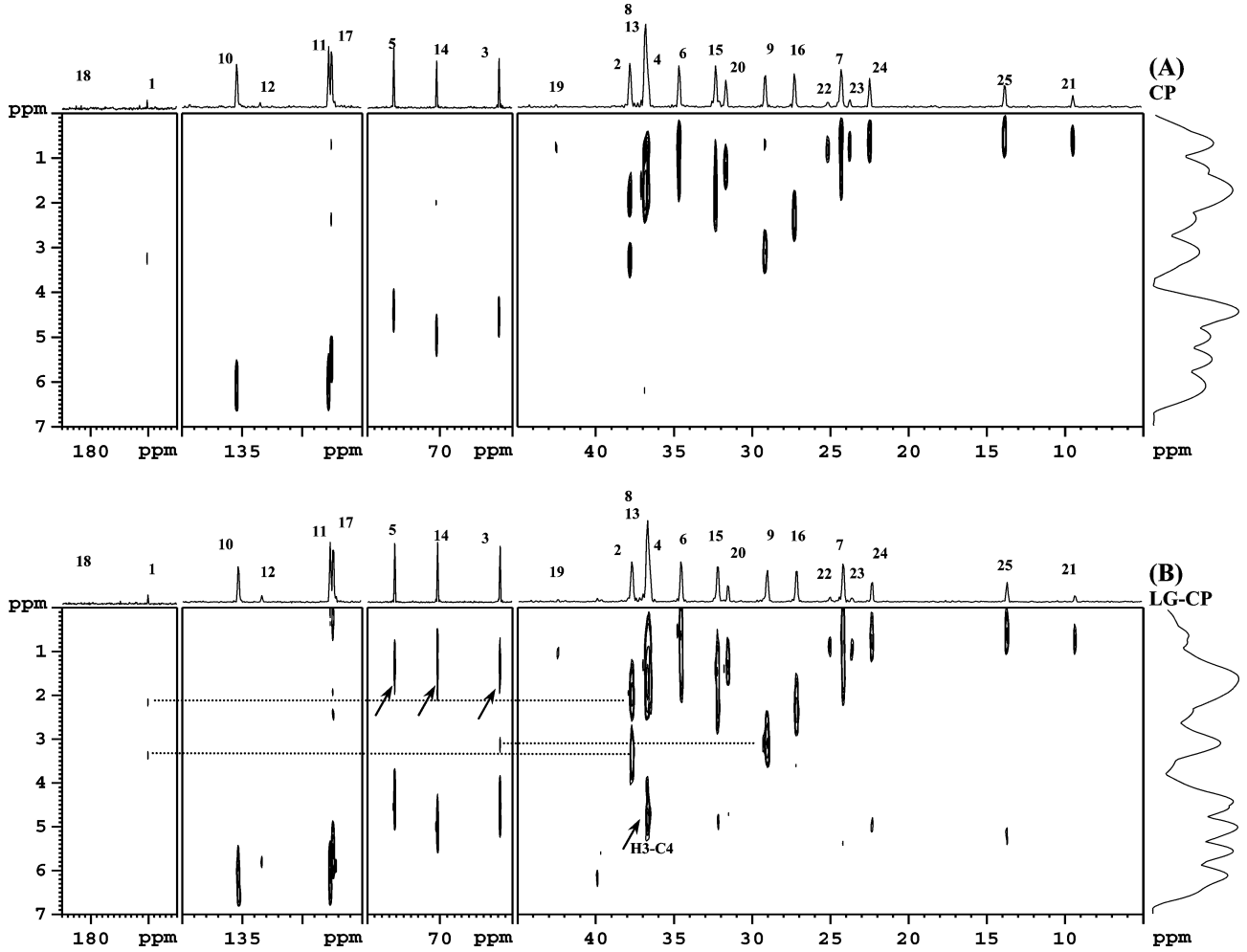

Figure 4. $^{1}H-^{13}C$ HETCOR (A) and LG-CP HETCOR (B) spectrum of simvastatin. Scans (56) for each of the 128 increments in t_1 were acquired. Duration of on-resonance and off-resonance spin lock was 100 μs. ^{1}H and ^{13}C projections are depicted in the upper and right side of 2D spectra. QSINE window function was used for processing in the F_1 dimension.

relatively weak. (Intermolecular hydrogen bonding follows from X-ray diffraction data with interatomic distance ca. 2.9 Å; see Figure 8.)

$^{1}H-^{13}C$ Dipolar Oscillation (Selectivity of Polarization Transfer). Because of the spectral overlap in the ^{1}H chemical shift dimension, only a part of coherences apparent in 2D spectra can be quite precisely assigned. Several cross peaks are not completely resolved due to the partial overlap of the ^{1}H NMR responses of neighboring protons that contribute to polarization transfer to a particular carbon. The most prominent example is the correlation signal reflecting polarization transfer from protons (H5) and (H14) to carbon (C7) (Figure 5B). This gives a single signal centered between both expected ^{1}H resonances. The position of this cross peak is independent of mixing time, because $^{1}H-^{13}C$ distance is almost equal for both spin pairs (ca. 2.75 Å). In the case where $^{1}H-^{13}C$ distances of both spin pairs are more different (e.g., H3−C6 and H5−C6, 4.6 and 2.1 Å), the position of correlation signal depends on the duration of LG-CP because the time evolution of both coherences is not exactly the same. In general we do not observe continuous build-up of correlation signals but rather oscillation in signal intensity.

Recently a LG-CP experiment under fast MAS was analyzed as a new tool for measuring dipolar coupling. As mentioned above, under this condition, the $^{1}H-^{1}H$ homonuclear dipolar interactions are suppressed. If the effective field strength, $\omega_{\mathrm{eff}} = \gamma_H B_{1\mathrm{eff}}$, is matched to the *S*-spin spin-lock field strength, $\omega_{1S} = \gamma_S B_{1S}$, by $\omega_{\mathrm{eff}} - \omega_{1S} = \pm\omega_r$, then the ^{1}H-*S* heteronuclear dipolar interaction is maintained and scaled by a factor of sin(54.7°). By incrementing the LG-CP contact time (i.e., 2D HETCOR is extended into 3D dipolar correlation experiment), the dipolar interactions are measured in indirect dimensions and resolved according to ^{1}H and *S*-spin isotropic chemical shift.

Although the resolution in ^{1}H dimension does not allow separation of all overlapping proton contributions (e.g., above-mentioned signal (H3/H5−C6) at 34.7 and 4.5 ppm), the observed oscillation of the signal intensity allows resolution of both contributions through analysis of the time evolution. In general, the time dependencies of the $^{1}H-^{13}C$ correlation signals, obtained during LG-CP, provide after Fourier transformation (FT) accurate dipolar spectra because rotor−asynchronous measurements can use long evolution time. Because of the enhanced selectivity of polarization transfer in 2D HETCOR, the number of interacting spins is restricted at most to 3−4 ^{1}H atoms correlating with one carbon atom as followed from inspection of X-ray diffraction data. This makes it possible to analyze and simulate dipolar spectra in detail because precise evaluation of the spin behavior requires a multispin calculation. Successful analysis of a seven-spin system, including one carbon and six protons, using Floquet theory has been recently reported.[17] It has been also shown that LG-CP MAS experiments can be well described by the effective time-independent Hamil-

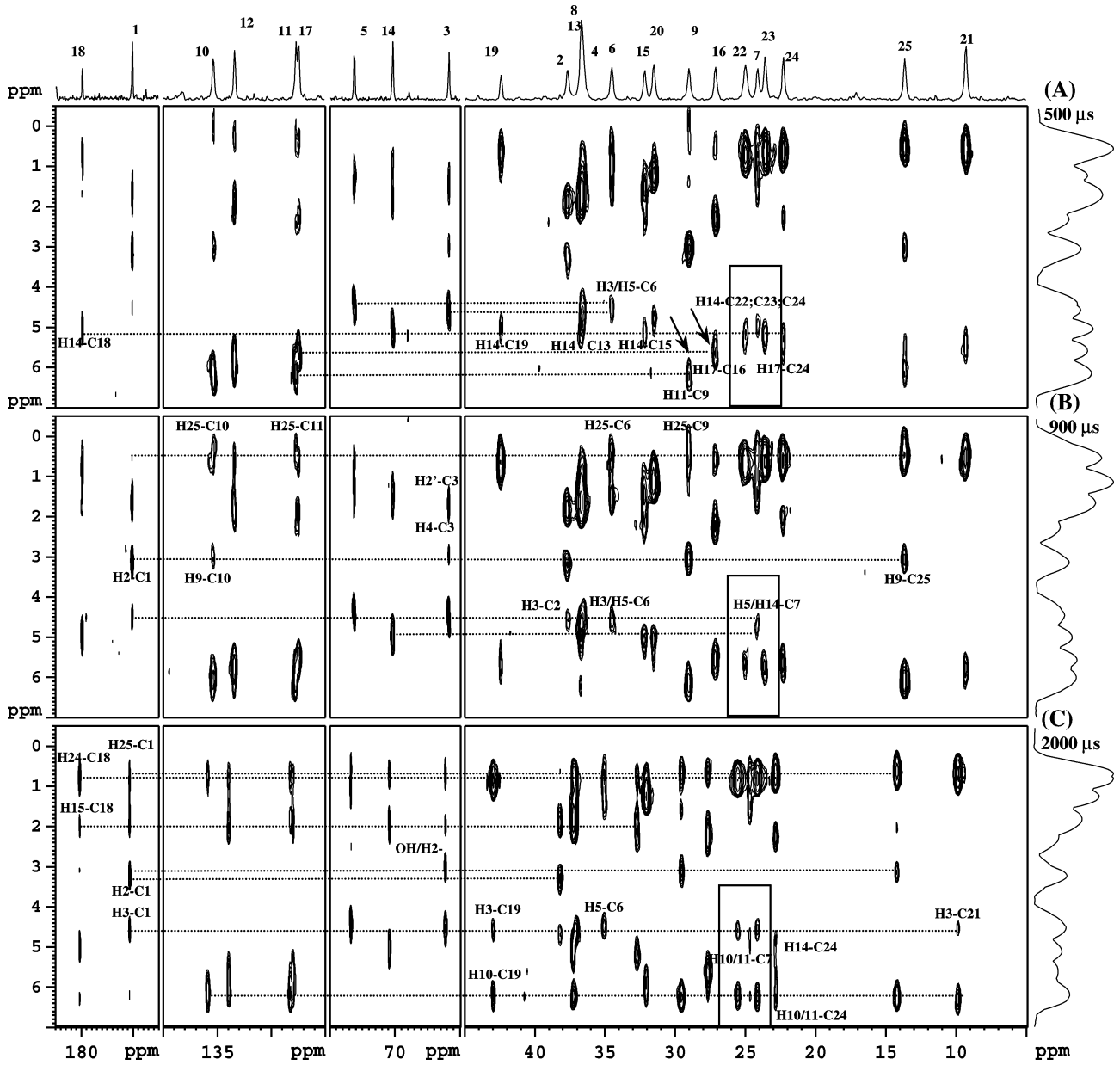

Figure 5. $^{1}H-^{13}C$ LG-CP HETCOR spectra of simvastatin. Scans (56) for each of the 128 increments in t_1 were acquired. Duration of off-resonance spin lock was 0.5, 0.9, and 2 ms for A, B and C, respectively. The dashed lines mark the ^{1}H NMR chemical shift and assist in the assignment of overlapping heteronuclear coherences.

tonian, which allows enlarging of the size of the spin system that can be efficiently studied numerically.[18]

Analysis of the correlation pattern is a bit complicated for the mobile ester tail of simvastatin. Although X-ray diffraction data propose significant disorder (Figure 6), we observe only one set of very narrow signals with a line width less than 15 Hz in this part of the molecule in the ^{13}C CP/MAS NMR spectrum. This indicates that inhomogeneous line broadening resulting from variation in a local electronic environment is almost negligible as the result of rapid motion of this ester unit. High-amplitude motion indicated by CPPI is confirmed by $^{1}H-^{13}C$ dipolar spectra measured by incremented a LG-CP experiment, indicating that heteronuclear dipolar interaction in the CH_2 unit (20) is comparable with dipolar $^{1}H-^{13}C$ coupling within rapidly rotating methyl group (Figure 7).

Consequently in 2D HETCOR spectra, we observe formation of a wide range of long-range correlation signals with significantly oscillating intensity (see small rectangle sections in parts A−C of Figure 5). This oscillation reflects not only the time evolution of particular coherence depending on interatomic distance but also molecular motion, i.e., changes of the position of a given group in time and consequently changes in probability of polarization transfer pathways. The correlation pattern indicates that the motion of this unit has the form of jumps between several preferred conformations. Although these correlation signals provide qualitative information about the geometry of the motion, accurate interatomic distance cannot be evaluated from their intensity and time oscillation.

Thus taking into account all these transfer processes, the total number of heteronuclear $^{1}H-^{13}C$ coherences detected in HETCOR spectra of simvastatin is more than 80. In addition to 25 one-bond correlations, we observe about 45 through-space $^{1}H-^{13}C$ contacts from which approximately one-half reflects structurally important long-range coherences between remote structure units. Consequently this technique provides valuable structural data almost comparable with information about $^{13}C-^{13}C$ distances obtained by, e.g., proton-driven spin-diffusion experiment (PDSD), which is, however, at natural isotopic

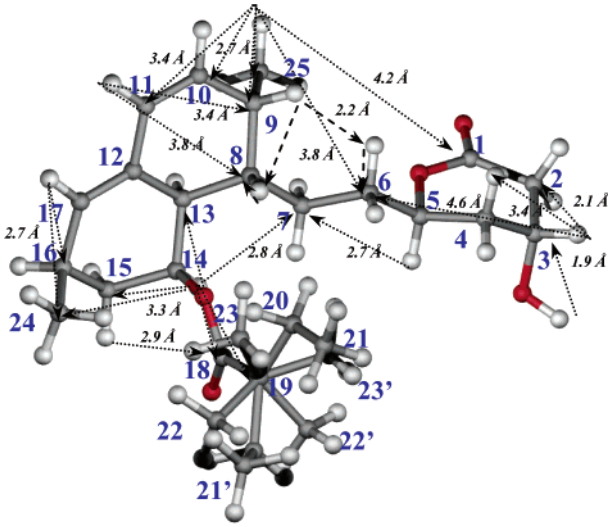

Figure 6. Conformation of a single molecule of simvastatin and proposed disorder of an ester tail (X-ray diffraction data).[21] Detected interatomic $^{1}H-^{13}C$ contacts are marked by arrows. Presented interatomic distances are approximate values as positions of hydrogen atoms were not refined.[21]

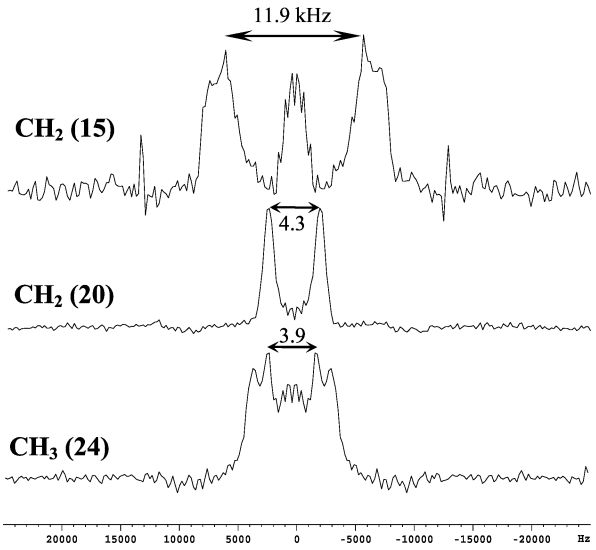

Figure 7. $^{1}H-^{13}C$ LG-CP dipolar spectra of CH_2 groups (15 and 20) and CH_3 (25). 200 increments of LG-CP with 10 μs dwell time were used. Motional averaging of $^{1}H-^{13}C$ dipolar coupling within CH_2 (20) and CH_3 (25) units is quite apparent.

abundance very time consuming and impractical, because series of spectra with various mixing time must be recorded to observe time evolution of correlation pattern.

Intermolecular vs Intramolecular Interactions. A crucial step for a reconstitution of a structural model of every crystalline material is the resolution of inter- and intramolecular $^{1}H-^{13}C$ interactions in HETCOR spectra. Recently it has been demonstrated that high-field correlation spectroscopy provides deep access to intermolecular correlations. The heteronuclear correlation of hydrocarbons especially favors the detection of intermolecular $^{1}H-^{13}C$ interaction, since protons are located at the exterior of molecule.[23] It is assumed that intermolecular $^{1}H-^{13}C$ correlation involves polarization transfer over large distances from 4 up to 5 Å. This corresponds with heteronuclear dipolar couplings of ca. 200−100 Hz, for which evolution requires a long transfer time. That is why for each assigned cross peak we measured all possible intra- and intermolecular ^{1}H-^{13}C contacts within enclosure sphere up to ca. 5 Å from central

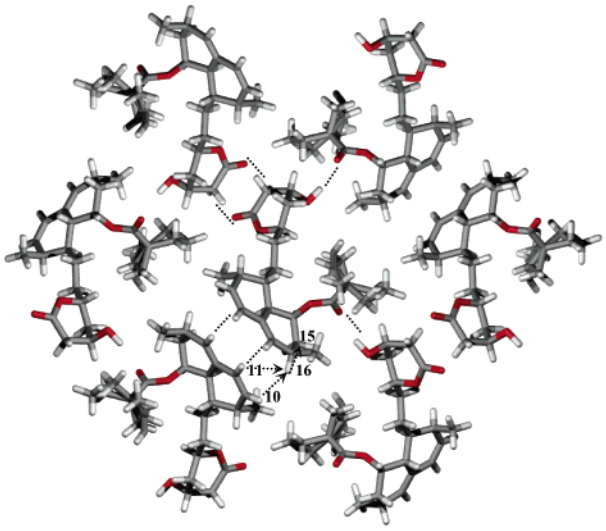

Figure 8. Molecular packing in crystalline simvastatin with a proposed disorder of an ester tail.[21] Examples of intermolecular contact detected by 2D HETCOR and NMR aggregation shifts are presented.

carbon using X-ray diffraction data. It is assumed that a dominant contribution of ^{1}H polarization to a given carbon atom originates from the closest ^{1}H nucleus, and thus detected cross peak predominantly reflects the shortest $^{1}H-^{13}C$ interatomic distance. For a rigid part of simvastatin molecule, we identify 10 signals in 2D HETCOR spectra that predominantly reflect intermolecular $^{1}H-^{13}C$ correlations (corresponding intramolecular contacts are larger). It must be stressed that five of the detected intermolecular $^{1}H-^{13}C$ contacts are significantly shorter than expected, less than 3.5 Å (H2−C1, 3.3 Å; H9−C1, 3.0 Å; H12−C11, 3.2 Å; H25−C16, 3.1 Å; H25−C17, 3.1 Å). The rest of the intermolecular correlations approximately fall within the expected region (3.5−5.1 Å). In some cases, corresponding intramolecular $^{1}H-^{13}C$ distances are too large to produce heteronuclear coherences. For instance, intramolecular $^{1}H-^{13}C$ distances for detected interactions H9−C1, H25−C16, or, H2−C18 are 5.4, 5.7, or 8.8 Å, respectively. However, the majority of detected heteronuclear interactions probably reflects both intra- and intermolecular polarization transfer events because both $^{1}H-^{13}C$ distances are smaller than 5 Å, the latter usually being less than 2 times the former ones. In principle, these contributions can be resolved after FT of the time evolution of cross-peak intensity during incremented spin lock if the distance of the more remote proton is at lest 1.2−1.4 times that of the nearer one.[18] If the differences in intra- and intermolecular distances are smaller, both contributions cannot be resolved (e.g., H11−C13, 3.44 and 3.42 Å, respectively). Fortunately, we have found by analysis of X-ray diffraction data that more than 70% of detected heteronuclear interactions in crystalline simvastatin fulfill this condition and thus contributions of inter- and intramolecular interactions could be in principle resolved. However, quite unambiguous separation of inter- and intramolecular contribution still remains open.

As no sharp border in distances between inter- and intramolecular correlations was found, additional indication of short-range intermolecular interaction by NMR aggregation shifts is promising. For instance, the shortest intermolecular contacts C1−H9 (2.97 Å) or C17−H25 (3.08 Å) are reflected by the largest ^{13}C and ^{1}H NMR aggregation shifts (3.61, 2.03, and −1.21 ppm or 2.39 and 0.33 ppm, respectively, see Table 1). From this follows that the detailed analysis of time evolution of heteronuclear coherences under LG-CP followed by careful simulation together with carbon and proton NMR aggregation

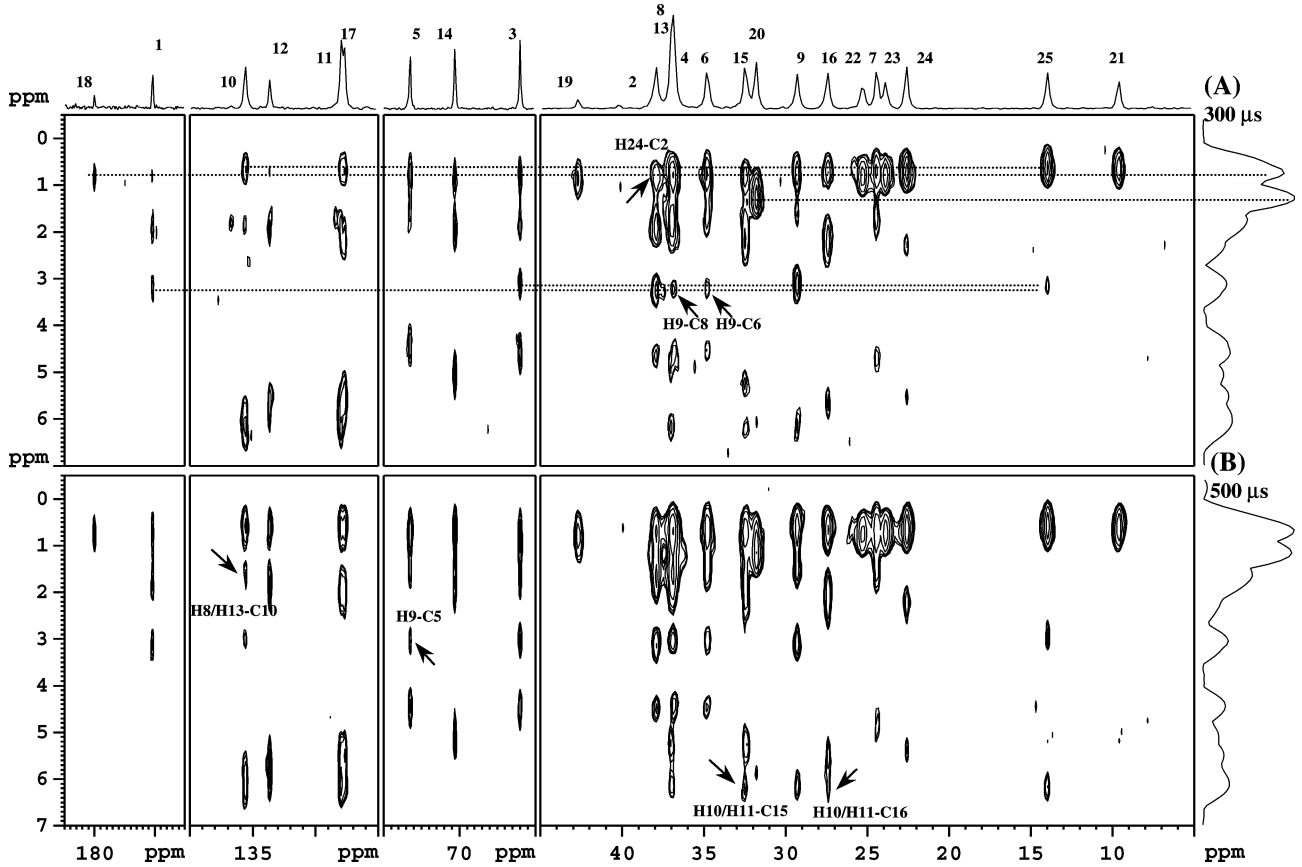

Figure 9. $^{1}H-^{13}C$ HETCOR spectra of simvastatin. Scans (56) for each of the 128 increments in t_1 were acquired. Duration of on-resonance spin lock was 300 and 500 μs for A and B, respectively.

shifts can provide the required geometrical restraints to calculate conformation and mutual orientation of crystallized molecules of simvastatin and related compounds.

$^{1}H-^{1}H$ Polarization Transfer. From 2D HETCOR spectra measured without suppression of ^{1}H spin diffusion during CP (Figure 9), it is clear that during on-resonance CP, transverse dephasing of CH and CH_2 coherences is much faster than that of rapidly rotating methyls and the CH_2 (20). Consequently, these hydrogen atoms become the main source of proton magnetization transferred to carbons, and their signals dominate in ^{1}H projection of 2D HETCOR spectra.

Evidently, we lost part of the long-range correlation signals involving transfer of ^{1}H polarization from CH and CH_2 to carbonyls C1 and C18 as well as quaternary carbon C19 and other rapidly moving carbon atoms (C22, C23, etc.). This reflects truncation of weak heteronuclear dipolar interactions by more intensive homonuclear $^{1}H-^{1}H$ couplings.

On the other hand, we observe formation of additional coherences corresponding to $^{1}H-^{1}H$ transfer. Behind the contacts between neighboring protons (correlation H9−C8 mediated by hydrogen H8, Figure 6), there are several long-range interactions that provide additional geometrical constraints. For instance, intramolecular correlation between hydrogen atom H9 and carbon atom C6 mediated by directly bonded proton H6 (Figure 6) as well as intermolecular correlation between hydrogen atoms H11/H10 and carbon atoms C15 and C16 (Figure 8). In principle, the time evolution of these interactions could be analyzed with respect to $^{1}H-^{1}H$ interatomic distances. However, as evolution of $^{1}H-^{13}C$ and $^{1}H-^{1}H$ coherences in the 2D HETCOR experiment is mixed and can be hardly resolved, for measurement of interatomic distances, it is necessary to increase selectivity of experiments for instance using 3D $^{1}H-^{1}H-^{13}C$ correlation experiment proposed by L. Elmsly et al.[27]

Conclusion

In this contribution, we tried to demonstrate the potential of solid-state NMR techniques to study and determine the 3D structure of moderately sized spin systems at natural isotopic abundance. Through-bond and through-space solid-state NMR correlation experiments (CP-INADEQUATE, $^{1}H-^{13}C$ HETCOR, $^{1}H-^{13}C$ MAS-*J*-HMQC) are presented on crystalline simavastatin ($C_{25}H_{38}O_5$).

(i) Because of the ideal organization of molecules in a crystal unit resulting in narrow ^{13}C NMR signals and because of the optimization of high-power decoupling, refocused $^{13}C-^{13}C$ CP-INADEQUATE provides a full correlation spectrum within a day of acquisition. Complete unambiguous ^{1}H and ^{13}C signal assignment was achieved by $^{1}H-^{13}C$ MAS-*J*-HMQC and dipolar heteronuclear correlation spectroscopy.

(ii) $^{1}H-^{13}C$ HETCOR with LG-CP was used to promote long-range heteronuclear polarization transfer. We observe significant oscillation in the buildup of correlation signals. For a rigid part of the molecules, this oscillation corresponds to the strength of dipolar coupling while for a rapidly moving ester structure group also reflects molecular motion. The total number of heteronuclear $^{1}H-^{13}C$ coherences detected in HETCOR spectra of simvastatin is more than 80. In addition to 25 one-bond correlations, we observed ca. 45 through-space $^{1}H-^{13}C$ contacts from which approximately one-half reflect long-range coherences between more remote structure units, which are suitable for structure determination.

(iii) No sharp border between inter- and intramolecular correlations was found. The range of intermolecular $^{1}H-^{13}C$

distances detected by correlation signals is 3.0−5.1 Å. Short-range intermolecular interactions are indicated by significant ^{13}C and ^{1}H NMR aggregation shifts. In general, correlation signals should be considered as a collective contribution of inter- and intramolecular polarization transfer events.

(iv) Because of the high selectivity and resolution of 2D LG-CP HETCOR, the number of protons interacting with one carbon reflected by a single cross peak does not exceed 3−4. This permits simulation of the observed oscillation of signal intensity during LG-CP with respect to $^{1}H-^{13}C$ dipolar coupling constants.

(v) Formation of additional coherences indicating $^{1}H-^{1}H$ polarization transfer providing further geometrical constraints was observed applying on-resonance CP as a mixing in 2D HETCOR.

From this follows that the detailed analysis of time evolution of hetero- and homonuclear $^{1}H-^{13}C$ and $^{1}H-^{1}H$ coherences under various conditions followed by careful simulation used in conjunction with NMR aggregation shifts can provide required geometrical restraints. It is clear that skillful execution and careful interpretation of modern solid-state NMR techniques can lead to a complete structure, i.e., conformation and mutual orientation of crystallized molecules of simvastatin and other related compounds. This attempt is currently in progress.

Acknowledgment. The authors thank the Grant Agency of the Czech Republic for financial support (Grant B4050203).

Supporting Information Available: Interatomic distances $^{13}C-^{1}H$, determined from X-ray diffraction data, including all possible intramolecular and intermolecular contacts and the corresponding number of potentially interacting ^{1}H atoms around the ^{13}C carbon atom within an enclosure sphere up to 5.1 Å as reflected by cross peaks in 2D $^{1}H-^{13}C$ LG-CP HETCOR NMR spectra. This material is available via the Internet at http://pubs.acs.org.

References and Notes

(1) Aue, W. P.; Bartholdi, E.; Ernst, R. R. *J. Chem. Phys.* **1975**, *64*, 2229.
(2) Müller, L. *J. Am. Chem. Soc.* **1979**, *101*, 4481.
(3) Bax, A.; Freeman, R.; Frenkiel, T. A. *J. Am. Chem. Soc.* **1981**, *103*, 2102.
(4) Baddrus, J.; Bauer, H. *Angew. Chem., Int. Ed. Engl.* **1987**, *26*, 625.
(5) Baldus, M.; Meier, B. H. *J. Magn. Reson.* **1996**, *118*, 65.
(6) Baldus, M.; Iuliucci, R. J.; Meier, B. H. *J. Am. Chem. Soc.* **1997**, *119*, 1121.
(7) Lesage, A.; Sakellariou, D.; Steuernagel, S.; Emsley, L. *J. Am. Chem. Soc.* **1998**, *120*, 13194.
(8) Lesage, A.; Emsley, L. *J. Magn. Reson.* **2001**, *148*, 449.
(9) Lesage, A.; Auger, C.; Caldarelli, S.; Emsley, L. *J. Am. Chem. Soc.* **1997**, *119*, 7867.
(10) Lesage, A.; Bardet, M.; Emsley, L. *J. Am. Chem. Soc.* **1999**, *121*, 10987.
(11) Kono, H.; Erata, T.; Takai, M. *Macromolecules* **2003**, *36*, 5131.
(12) Olsen, R. A.; Struppe, J.; Elliot, D. W.; Thomas, R. J.; Mueller, L. J. *J. Am. Chem. Soc.* **2003**, *125*, 11784.
(13) De Paëpe, G.; Giraud, N.; Lesage, A.; Hodgkinson, P.; Böckmann, A.; Emsley, L. *J. Am. Chem. Soc.* **2003**, *125*, 13938.
(14) Lee, M.; Goldburg, W. I. *Phys. Rev. A* **1965**, *140*, 1261.
(15) Bielecki, A.; Kolbert, A. C.; Levitt, M. H. *Chem. Phys. Lett.* **1989**, *155*, 341.
(16) Vinogradov, E.; Madhu, P. K.; Vega, S. *Chem. Phys. Lett.* **1999**, *314*, 443.
(17) van Rossum, B. J.; de Groot, C. P.; Ladizhansky, V.; Vega, S.; de Groot, H. J. M. *J. Am. Chem. Soc.* **2000**, *122*, 3465.
(18) Ladizhansky, V.; Vega, S. *J. Chem. Phys.* **2000**, *112*, 7158.
(19) Wu, X.; Burns, T.; Zilm, K. W. *J. Magn. Reson. A* **1994**, *111*, 29.
(20) Lesage, A.; Steuernagel, S.; Emsley, L. *J. Am. Chem. Soc.* **1998**, *120*, 7095.
(21) Čejka, J.; Kratochvíl, B.; Císařová, I.; Jegorov, A. *Acta Crystallogr.* **2003**, *C59*, 428.
(22) Bennet, A. E.; Rienstra, C. M.; Auger, M.; Lakshmi, K. V.; Griffin, R. G. *J. Chem. Phys.* **1995**, *103*, 6951.
(23) van Rossum, B. J.; Schulten, E. A. M.; Raap, J.; Oschkinat, H.; de Groot, H. J. M. *J. Magn. Reson.* **2002**, *155*, 1.
(24) Zilm, K. W. *The Encyklopedia of NMR*; John Willey & Sons: London, 1997.
(25) De Paëpe, G.; Hodgkinson, P.; Emsley, L. *Chem. Phys. Lett.* **2003**, *376*, 259.
(26) Castellani, F.; van Rossum, B.; Diehl, A.; Schubert, M.; Rehbein, K.; Oschkinat, H. *Nature* **2002**, *420*, 98.
(27) Sakellariou, D.; Lesage, A.; Emsley, L. *J. Am. Chem. Soc.* **2001**, *123*, 5604.